bidentate ligands and the conformations of the rings formed by these ligands are determined by a large number of intermolecular contacts.

Acknowledgment. The research performed at Oak Ridge National Laboratory was sponsored by the Division of Material Sciences, Office of Basic Energy Sciences, U.S. Department of Energy, under Contract W-7405-eng-26 with the Union Carbide Corp. The research performed at the University of Georgia was supported partially by the U.S. Air Force Office of Scientific Research under Grant AFOSR-75-2869.

Registry No. $\{CH_3N[P(OCH_3)_2]_2\}_2Co_2(CO)_4$, 81011-78-1; $Co_2(CO)_8$, 10210-68-1; $CH_3N[P(OCH_3)_2]_2$, 34244-05-8; $CH_3N(PCl_2)_2$, 17648-16-7; methanol, 67-56-1.

Supplementary Material Available: A table of coordinates and thermal parameters of the hydrogen atoms and a listing of observed and calculated values of F^2, with estimated standard errors of the former (22 pages). Ordering information is given on any current masthead page.

Contribution from the Department of Chemistry,
University of Nevada, Reno, Nevada 89557, and the Laboratoire CNRS-SNPE, 94320 Thiais, France

Intra- and Intermolecular Equilibria and Their Pertinence to the Mechanism of Cis–Trans Isomerization of L_2PtX_2 Complexes: Four- and Five-Coordinate Platinum Phosphole Complexes

J. JEFFREY MacDOUGALL,[1a] JOHN H. NELSON,*[1a] and FRANCOIS MATHEY*[1b]

Received August 20, 1981

A series of platinum(II) complexes of the type L_2PtX_2 (L = 1-R-3,4-dimethylphosphole; R = $-CH_3$, $-n-C_4H_9$, $-t-C_4H_9$, $-C_6H_5$, $-CH_2C_6H_5$; X = Cl^-, Br^-, I^-) have been prepared and characterized by elemental analyses, physical properties, conductance measurements, infrared spectroscopy, and ^1H, $^{13}C\{^1H\}$, $^{31}P\{^1H\}$, and $^{195}Pt\{^1H\}$ NMR spectroscopy. All complexes are nonelectrolytes in chloroform and methanol solutions and most possess the cis geometry in solution as well as in the solid state. Variable-temperature $^{31}P\{^1H\}$ and $^{195}Pt\{^1H\}$ NMR spectroscopy and conductance studies of the equilibrium $L_2PtX_2 + L \rightleftharpoons L_3PtX_2$ have been analyzed in terms of intra- and intermolecular equilibria of the pentacoordinate species L_3PtX_2. The formation of L_3PtX_2 is enthalpy favored and entropy disfavored. The relative thermodynamic stability of the L_3PtX_2 complexes is a function of ligand steric bulk; the smaller ligand gives the greater stability. The stereochemical rigidity of the L_3PtX_2 complexes is inversely proportional to ligand steric bulk: the larger the ligand, the more rigid the L_3PtX_2 complex. The relationship of these observations to the mechanism of cis–trans isomerization of L_2MX_2 (M = Pd, Pt) is discussed. Coordination chemical shift relationships of the form $\Delta\delta(^{31}P) = A[\delta(^{31}P_{ligand})] + B$ were found for the four-coordinate L_2PtX_2 complexes and for both of the magnetically inequivalent phosphole ligands in the five-coordinate L_3PtX_2 complexes. The complexes *cis*-$L_2PtBrCl$, which are intermediates in the bromide ligand substitution reactions of *cis*-L_2PtCl_2, were isolated and characterized. They demonstrate that anion ligand substitution of *cis*-L_2PtCl_2 complexes occurs with complete retention of configuration. This is direct evidence of the kinetic trans effect. In contrast, iodide substitution of L_2PtCl_2 to produce L_2PtI_2 is accompanied by some cis–trans isomerization, as mixtures of *cis*- and *trans*-L_2PtI_2 are formed in these reactions. This is evidence of the thermodynamic trans effect. The $L_2PtBrCl$ complexes react with excess L to form $L_3PtBrCl$ rather than $[L_3PtBr]Cl$ or $[L_3PtCl]Br$ in support of the contention that the equilibrium can be best described as $L_2PtX_2 + L \rightleftharpoons L_3PtX_2$ and not as $L_2PtX_2 + L \rightleftharpoons [L_3PtX]X$. Thus, five-coordinate complexes and not ionic four-coordinate complexes are formed in solutions of L_2PtX_2 upon addition of excess ligand (L). The implications of this in regard to consecutive anion displacement for isomerization of L_2PtX_2 complexes is discussed.

Introduction

Much effort[2-18] has been expended toward understanding the mechanisms of ligand substitution and isomerization of square-planar transition-metal complexes. While it is becoming clearer that pentacoordinate species are involved[2,4,9,16,19-21] in these processes, there is little information[18] regarding the solution structure and reactivity of pentacoordinate Pd(II) and Pt(II) ML_3X_2 complexes. Sterically undemanding ligands that possess both strong σ-donor and π-acceptor abilities are held[14,22,23] to be an important stabilizing influence on these pentacoordinate complexes. Of the few d^8 pentacoordinate species that have been characterized, most have involved phospholes[24,25] or trimethylphosphine.[26] Superficially, phosphole (I, R^1 = R = H) is very similar to the

---

(1) (a) University of Nevada. (b) Laboratoire CNRS-SNPE.

(2) Basolo, F.; Pearson, R. G. "Mechanisms of Inorganic Reactions", 2nd ed.; Wiley: New York, 1967.

(3) Haake, P.; Pfeffer, R. M. *J. Chem. Soc. D* **1969**, 1330; *J. Am. Chem. Soc.* **1970**, *92*, 5243.

(4) Haake, P.; Pfeiffer, R. M. *J. Am. Chem. Soc.* **1970**, *92*, 4996.

(5) Faraone, G.; Ricevuto, U.; Romeo, R.; Trozzi, M. *J. Chem. Soc. A* **1971**, 1877.

(6) Cooper, D. G.; Powell, J. *Can. J. Chem.* **1973**, *51*, 1634.

(7) Cooper, D. G.; Powell, J. *J. Am. Chem. Soc.* **1973**, *95*, 1102.

(8) Redfield, D. A.; Nelson, J. H. *Inorg. Chem.* **1973**, *12*, 15.

(9) Louw, W. J. *J. Chem. Soc., Chem. Commun.* **1974**, 353.

(10) Redfield, D. A.; Nelson, J. H. *J. Am. Chem. Soc.* **1974**, *96*, 6219.

(11) Powell, J.; Cooper, D. G. *J. Chem. Soc., Chem. Commun.* **1974**, 749.

(12) Redfield, D. A.; Nelson, J. H.; Henry, R. A.; Moore, D. W.; Jonassen, H. B. *J. Am. Chem. Soc.* **1974**, *96*, 6298.

(13) Redfield, D. A.; Cary, L. W.; Nelson, J. H. *Inorg. Chem.* **1975**, *14*, 50.

(14) Verstuyft, A. W.; Cary, L. W.; Nelson, J. H. *Inorg. Chem.* **1976**, *15*, 3161.

(15) Romeo, R.; Minniti, D.; Trozzi, M. *Inorg. Chem.* **1976**, *15*, 1134.

(16) Louw, W. J. *Inorg. Chem.* **1977**, *16*, 2147.

(17) Romeo, R. *Inorg. Chem.* **1978**, *17*, 2040.

(18) Favez, R.; Roulet, R.; Pinkerton, A.; Schwarzenbach, D. *Inorg. Chem.* **1980**, *19*, 1356.

(19) Cattalini, L. *Prog. Inorg. Chem.* **1970**, *13*, 263.

(20) Hartley, F. R. *Chem. Soc. Rev.* **1973**, *2*, 163.

(21) Langford, C. H.; Gray, H. B. "Ligand Substitution Processes"; W. A. Benjamin: New York, 1965.

(22) Wood, J. S. *Prog. Inorg. Chem.* **1972**, *16*, 227.

(23) Burdett, J. K. *Inorg. Chem.* **1977**, *16*, 3013.

(24) Chui, K. M.; Powell, H. M. *J. Chem. Soc., Dalton Trans.* **1974**, 1879.

(25) Chui, K. M.; Powell, H. M. *J. Chem. Soc., Dalton Trans.* **1974**, 2117.

(26) Merle, A.; Dartiguenave, M.; Dartiguenave, Y.; Dawson, I. W.; Gray, H. B. *J. Coord. Chem.* **1974**, *3*, 199. Dawson, I. W.; Bryant, T. I.; Robinson, N. R.; Merle, A.; Dartiguenave, M.; Dartiguenave, Y.; Gray, H. B. *J. Am. Chem. Soc.* **1974**, *96*, 4428. Meier, P.; Merbach, A. E.; Dartiguenave, M.; Dartiguenave, Y. *Ibid.* **1976**, *98*, 6402. Dartiguenave, M.; Dartiguenave, Y.; Gleizes, A.; Saint-Joly, C.; Galy, J.; Meier, P.; Merbach, A. E. *Inorg. Chem.* **1978**, *17*, 3503.

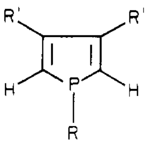

I, $R' = H$
II, $R' = CH_3$
IIa, $R = CH_3$
b, $R = n\text{-}C_4H_9$
c, $R = t\text{-}C_4H_9$
d, $R = C_6H_5$
e, $R = CH_2C_6H_5$

aromatic pyrrole molecule, and studies regarding the possible aromatic character of phosphole and its derivatives have been reviewed.[27] The interaction of the phosphorus lone pair with the ring butadiene π system would clearly affect the donor character of the phosphorus atom. We recently demonstrated[28,29] that 1-substituted 3,4-dimethylphosphole (II) forms bonds with Pd(II) of comparable or greater strength than those between Pd(II) and structurally similar phosphines. There is convincing evidence[29] for the involvement of pentacoordinate intermediates or transition states in the cis–trans isomerization of these Pd(II)–phosphole complexes. Square-planar Pt(II) complexes are more inert[2] toward ligand substitution than their Pd(II) counterparts, and we might expect the same trend for the pentacoordinate Pt(II) species as well, making them more amenable to study by NMR than the Pd(II) complexes. With this in mind we prepared and characterized the series L_2PtX_2 (L = IIa–e, X = Cl, Br, I) and investigated their solution behavior, both in solution alone and in solution in the presence of excess phosphole. We hoped through this study to be able to present a more unified picture of the isomerization mechanism of four-coordinate complexes.

Experimental Section

A. Reagents and Physical Measurements. Chemicals were reagent grade and were used as received or synthesized as described below. All solvents were dried when necessary by standard procedures and stored over Linde 4A molecular sieves. Melting points were determined on a Mel-Temp apparatus and are uncorrected.

Conductivity studies were performed as described previously.[28] The complexes are not electrolytes in CH_3OH and CH_2Cl_2 in the presence and absence of excess ligand.

Infrared spectra were recorded on a Perkin-Elmer 599 spectrophotometer as Nujol mulls between CsBr plates.

The ^1H, $^{13}C\{^1H\}$, $^{31}P\{^1H\}$, and $^{195}Pt\{^1H\}$ NMR spectra were recorded at 99.54, 25.00, 40.26, and 21.30 MHz, respectively, on a JEOL FX-100 spectrometer in the FT mode. Proton and carbon chemical shifts are downfield relative to internal Me_4Si, while the phosphorus chemical shifts are relative to 85% H_3PO_4. A positive value of $\delta(^{31}P)$ indicates a downfield position relative to that of the reference. Platinum-195 chemical shifts are referenced to the standard frequency[30] 21.4 MHz relative to the proton resonance of Me_4Si at exactly 100 MHz. NMR solvents were spectroscopic grade and were used as received from the manufacturer. Preparation of samples for NMR analyses has been described.[8]

Equilibrium constants for the equilibria $L_2PtX_2 + L \rightleftharpoons L_3PtX_2$ were obtained at various temperatures by integrating the areas under the appropriate $^{31}P\{^1H\}$ NMR signals for $CDCl_3$ solutions containing a 1:1 mole ratio of L and L_2PtX_2. Plots of ln K_{eq} vs. T^{-1} were treated by least-squares analyses to obtain ΔH^* and ΔS^*.

B. Syntheses. The phospholes were prepared by previously described methods[31] and were handled and allowed to react with other chemicals in a nitrogen atmosphere. The chloride complexes were prepared by reacting a 1:1 v/v ethanol–water solution of K_2PtCl_4 with twice the stoichiometric amount of the appropriate phosphole dissolved in ethanol and were precipitated upon addition of excess water. The bromides and iodides were prepared by metatheses of the chloride complexes in ethanol. Care must be taken, especially in preparing the bromide complexes, that sufficient time is allowed for the metathesis reaction to go to completion (72 h to be safe) as platinum is robust; otherwise the mixed-halide species will be isolated in place of the desired homogeneous product (vide infra). The solvent was then removed on a rotary evaporator, and the residue was extracted with CH_2Cl_2, from which crystals ensued upon addition of hexane. The complexes were recrystallized from ethanol–water or acetone–water mixtures and were vacuum-dried at room temperature. Elemental analyses (Table I) were performed by Galbraith Laboratories, Knoxville, TN 37921.

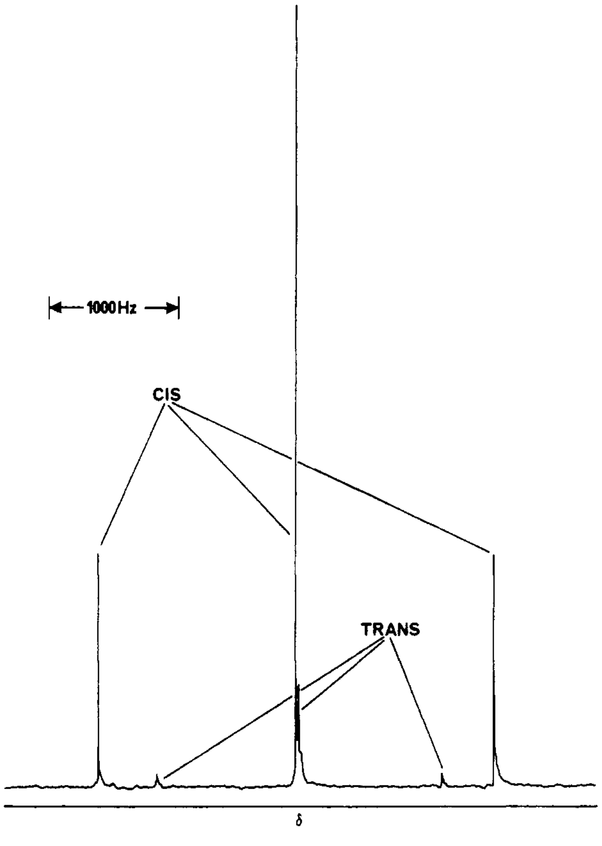

Figure 1. $^{31}P\{^1H\}$ NMR of $(1,3,4\text{-trimethylphosphole})_2PtI_2$ showing cis and trans isomers in CH_2Cl_2 at 300 K.

Results and Discussion

I. Four-Coordinate Complexes. Elemental analyses, spectroscopic data, and the absence of solution conductance all indicate that phospholes IIa–e form typical square-planar L_2PtX_2 complexes that do not readily dissociate in either CH_2Cl_2 or CH_3OH solutions. Infrared spectroscopy (Table II) shows that these complexes are primarily cis in the solid state, as indicated[32] by the appearance of two bands for ν(Pt–X) and ν(Pt–P). Proton NMR (Table III) and $^{13}C\{^1H\}$ NMR (Table IV) exhibit line shapes and coupling constants that are very similar to those exhibited by the analogous Pd(II) phosphole complexes[28] and suggest that the cis complexes are the dominant species in solution. The $^{31}P\{^1H\}$ NMR and $^{195}Pt\{^1H\}$ NMR spectra (Table V) also indicate that the L_2PtX_2 complexes are predominantly cis in CH_2Cl_2 solution at 25 °C.

---

(27) Hughes, A. N. *Stud. Org. Chem. (Amsterdam)* **1979**, *3*. Mathey, F. *Top. Phosphorus Chem.* **1980**, *10*. Quin, L. D. "The Heterocyclic Chemistry of Phosphorus"; Wiley-Interscience: New York, 1981.

(28) MacDougall, J. J.; Nelson, J. H.; Mathey, F.; Mayerle, J. J. *Inorg. Chem.* **1980**, *19*, 709.

(29) MacDougall, J. J.; Mathey, F.; Nelson, J. H. *Inorg. Chem.* **1980**, *19*, 1400.

(30) Goggin, P. L.; Goodfellow, R. J.; Haddock, S. R.; Taylor, B. F.; Marshall, I. R. H. *J. Chem. Soc., Dalton Trans.* **1976**, 459.

(31) Mathey, F.; Mankowski-Favelier, R. *Org. Magn. Reson.* **1972**, *4*, 171. Mathey, F. *Tetrahedron* **1972**, *28*, 4171.

(32) Assignments were made consistent with those of: Duddell, D. A.; Goggin, P. L.; Goodfellow, R. J.; Norton, M. G.; Smith, J. G. *J. Chem. Soc. A* **1970**, 545. Goggin, P. L.; Goodfellow, R. J.; Reed, F. J. S. *J. Chem. Soc., Dalton Trans.* **1972**, 1298. Reference 25.

Table I. Physical Data for the (1-R-3,4-dimethylphosphole)$_2$PtX$_2$ Complexes

					anal.			
					% C		% H	
R	X	color	% yield	dec pt, °C	calcd	found	calcd	found
CH_3	Cl	pale yellow plates	74.5	>320	32.46	32.48	4.25	4.37
n-C_4H_9	Cl	pale yellow plates	79.2	157-158	39.90	39.24	5.65	5.52
t-C_4H_9	Cl	colorless needles	89.3	>310 dec	39.90	39.39	5.65	5.61
$C_6H_5CH_2$	Cl	pale yellow needles	86.5	210-213	46.60	46.67	4.48	4.57
C_6H_5	Cl	pale yellow cubes	79.0	214-216	44.89	44.74	4.05	4.16
CH_3	Br	pale yellow needles	91.5	>300	27.70	27.56	3.62	3.46
n-C_4H_9	Br	pale yellow microcrystals	99.5	139-140	34.76	34.79	4.92	5.04
t-C_4H_9	Br	pale yellow plates	62.6	>300	34.76	34.58	4.92	4.86
$C_6H_5CH_2$	Br	pale yellow microcrystals	96.5	197-198	41.14	41.00	3.95	3.69
C_6H_5	Br	pale orange cubes	93.9	220-221	39.43	39.26	3.56	3.38
CH_3	I	orange needles	93.2	264-266	23.99	23.79	3.14	3.03
n-C_4H_9	I	orange microcrystals	54.8	128-130	30.60	30.51	4.33	4.18
t-C_4H_9	I	golden needles	98.5	. >300	30.60	30.82	4.33	4.22
$C_6H_5CH_2$	I	yellow needles	95.3	182-183	36.61	36.41	3.51	3.52
C_6H_5	I	golden needles	99.4	223-224	34.97	34.91	3.15	3.13

Table II. Infrared Spectral Data in the 200-600 cm^{-1} Range for (1-R-3,4-dimethylphosphole)$_2$PtX$_2$ (ν, cm^{-1})

R	X	ν(PtX)	ν(PtP)	other vib	geometry
CH_3	Cl	310, 285	441, 407	339, 398, 523, 545	cis
n-Bu	Cl	307, 283	468, 400	360, 478, 542, 571	cis
t-Bu	Cl	302, 285	435, 378	390, 464, 550, 571	cis
Ph	Cl	323, 291	407, 380	477, 501, 549, 581	cis
Bzl	Cl	315, 292	409, 339	400, 493, 528, 541, 570	cis
CH_3	Br	252, 210	440, 405	300, 336, 398, 520, 543	mostly cis and trans
n-Bu	Br	a	468, 400	298, 355, 365, 538, 580	cis
t-Bu	Br	230, 210	433, 375	298, 390, 463, 548, 570	cis
Ph	Br	270, 230	405, 378	307, 475, 498, 546, 570	cis
Bzl	Br	256, 230	407, 337	300, 490, 525, 540, 570	mostly cis and trans
CH_3	I	a	435, 402	335, 395, 514, 538	mostly cis and trans
n-Bu	I	a	460, 418	345, 355, 370, 435, 490, 520, 535, 550	cis
t-Bu	I	a	390	284, 365, 433, 460, 538, 560	trans
Ph	I	a	400, 380	478, 496, 542, 561	mostly cis and trans
Bzl	I	a	408, 334	370, 489, 522, 537, 570	cis

[a] Occurs below 225 cm^{-1} and is not observable on our instrument.

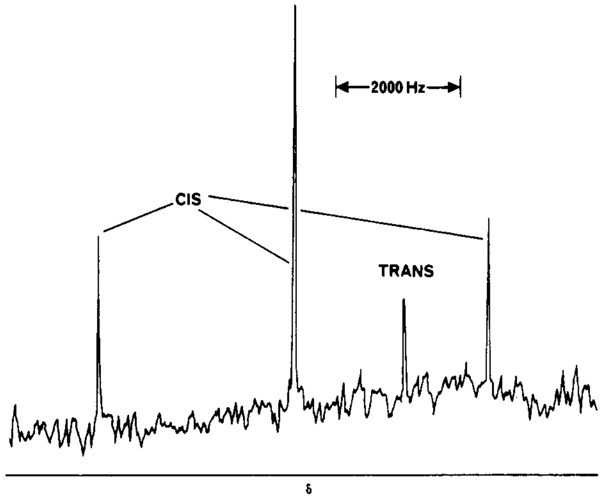

Figure 2. ^{195}Pt{^{1}H} NMR of (1-benzyl-3,4-dimethylphosphole)$_2$PtI$_2$ showing cis and trans isomers in CH$_2$Cl$_2$ at 300 K.

Figures 1 and 2 exhibit typical ^{31}P{^{1}H} and ^{195}Pt{^{1}H} NMR spectra, respectively, where both *cis*- and *trans*-L$_2$PtX$_2$ are present together in solution. For each isomer, the ^{31}P{^{1}H} spectrum typically shows a single resonance due to 66.2% of the phosphorus nuclei coordinated to platinum nuclei other than ^{195}Pt, with an overlapping doublet from the remaining 33.8% of the phosphorus nuclei coupled to ^{195}Pt ($I = {}^1/_2$),

Table III. ^{1}H NMR Data for the (1-R-3,4-dimethylphosphole)$_2$PtX$_2$ Complexes at 30 °C in CDCl$_3$[a]

		δ(^{1}H), line shape, "J_{PH}",[b] J_{PtH}				
R	X	phosphole ring CH_3	phosphole ring H	t-Bu CH_3	P-CH_3	benzyl CH_2
CH_3	Cl	2.11, s, 0, 10.3	6.42, d, 32.2, 16.0		1.75, d, 12.0, 40.8	
CH_3	Br	2.11, s, 0, 10.0	6.50, d, 32.9, NO		1.76, "t", 20.3, 48.0	
CH_3	I	2.05, s, 0, 10.0	6.78, t, 32.0, NO		1.75, t, 20.7, NO	
		2.08, s, 0, 10.0	6.62, d, 32.2, NO		1.90, d, 11.7, 32.0	
n-Bu	Cl	2.10, s, 0, 12.0	6.41, d, 30.8, 30.0			
n-Bu	Br	2.10, s, 0, 11.7	6.45, d, 30.8, NO			
t-Bu	Cl	2.11, s, 0, 11.4	6.59, d, 30.3, NO	1.15, d, 16.4, 0		
t-Bu	Br	2.09, s, 0, 11.2	6.67, d, 31.3, NO	1.17, d, 16.1, 0		
t-Bu	I	2.02, s, 0, 7.4	6.98, t, 29.1, NO	1.35, t, 15.3, 0		
Ph	Cl	2.00, s, 0, 11.5	6.40, d, 31.8, 24.0			
Ph	Br	1.99, s, 0, 11.0	6.48, d, 32.5, NO			
Ph	I	2.11, s, 0, 6.8	7.08, t, 32.0, NO			
		1.95, s, 0, 11.0	6.56, d, 32.0, NO			
Bzl	Cl	1.87, s, 0, 11.8	6.05, d, 30.5, NO			3.42, d, 12.5, 33.7
Bzl	Br	1.86, s, 0, 11.3	6.13, d, 30.5, NO			3.50, d, 12.7, 33.4
Bzl	I	1.84, s, 0, 10.6	6.24, d, 31.7, NO			3.64, d, 12.0, 33.4

[a] Chemical shifts in ppm relative to internal Me$_4$Si: s = singlet, d = doublet, t = triplet, "t" = non-1:2:1 triplet. [b] "J_{PH}" = $|{}^nJ_{PH} + {}^{n+2}J_{PH}|$, NO = not observed; all J values in hertz.

Table IV. Carbon-13 Data for (1-R-3,4-dimethylphosphole)$_2$PtX$_2$ Complexes[a]

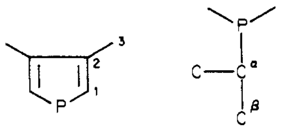

position	X	$\delta(^{13}C)$, $\vert{}^1J_{PC} + {}^3J_{PC}\vert$, $\vert{}^2J_{PtC}$					
		CH_3	*n*-Bu	*t*-Bu	Ph	Bzl	$(CH_3)_2PPh$
1	Cl	124.9 f, 64.7, 35.4	123.7 f, 63.5, 33.0	124.4 f, 58.6, 30.8	124.3 f, 67.1, 28.1	123.1, 63.5, 36.6	
	Br	126.0 f, 65.9, 37.8	124.8 f, 62.3, 34.2	126.0 f, 59.8, 31.7	125.4 f, 67.1, 29.3	124.3, 63.5, 39.1	
	I	127.0 f, 63.5, 36.6		128.3 t, 54.9, NO	127.8 f, 65.9, 29.3	126.3, 62.3, 37.9	
2	Cl	154.0 f, 12.2, 35.4	154.5 t, 11.0, 34.2	154.2 f, 11.0, 31.7	155.2 t, 13.4, 33.0	155.0 t, 12.2, 34.2	
	Br	NO	154.7 t, 12.2, NO	154.1 t, 9.8, 30.5	155.0 f, 12.2, 34.2	154.6 f, 12.2, NO	
	I	153.8 t, 13.4, 35.7		153.4 t, 12.2, NO	154.9 f, 12.2, NO	154.4 f, 11.0, NO	
3	Cl	18.6 t, 13.4, 40.3	18.6 f, 13.4, 36.6	18.5 t, 13.4, 35.4	18.5 t, 14.7, 42.7	18.5 t, 14.7, 34.2	
	Br	18.5 t, 14.7, 37.9	18.5 f, 13.4, NO	18.6 f, 13.4, NO	18.5 f, 14.7, 40.3	18.5 f, 14.7, 29.3	
	I	18.6 t, 13.4, 28.1		18.7 t, 11.0, NO	18.5 f, 13.4, NO	18.5 f, 13.4, NO	
α	Cl	12.5 f, 41.5, NO		36.1 f, 34.2, NO		34.5 f, 34.2, NO	
	Br	13.7 f, 41.5, NO		36.5 f, 33.0, NO		35.7 f, 34.2, NO	
	I	15.1 f, 41.5, 30.0		NO, NO, NO		37.3 f, 35.4, NO	
β	Cl			29.7 s, 14.7, NO			
	Br			30.3 s, 15.9, NO			
	I			31.1 s, NO, NO			
C_1 (Ph)	Cl				126.3 t, 71.4, NO		132.7 d, 64.7, NO
	Br				125.4 f, 67.1, 29.3		
	I				NO, NO, NO		
$-CH_3$	Cl						15.3 f, 46.4, 34.2
	Br						
	I						

[a] NO indicates that a signal was either not observed or not able to be assigned; s = singlet, d = doublet, t = triplet, f = five-line multiplet.

Table V. $^{31}P\{^1H\}$ and $^{195}Pt\{^1H\}$ NMR Spectral Data for L_2PtX_2

L = 1-R-3,4-dimethylphosphole

R	X	$\delta(^{31}P_{ligand})$[a]	$\delta(^{31}P_{complex})$[a]	$\Delta\delta(^{31}P)$[b]	$^1J_{PtP}$[a]	$\delta(^{195}Pt)$[c]	geometry
CH_3	Cl	−20.2	−2.1	18.1	3291	138	cis
n-Bu	Cl	−6.5	9	15.5	3301	96	cis
t-Bu	Cl	+27.5	39.7	12.2	3306	17	cis
Ph	Cl	−2.5	8.1	10.6	3345	50	cis
Bzl	Cl	−3.0	11.4	14.4	3381	71	cis
CH_3	Br	−20.2	−1.8	18.4	3236	−144	cis
n-Bu	Br	−6.5	9.3	15.8	3242	−198	cis
t-Bu	Br	+27.5	27.1	−0.4	3258	−312	cis
Ph	Br	−2.5	7.9	10.4	3268	−272	cis
Bzl	Br	−3.0	11.6	14.6	3325	−217	cis
CH_3	I	−20.2	−3.2	17.0	3079	−350	cis
CH_3	I	−20.2	−3.8	16.4	2217	−439	trans
t-Bu	I	+27.5	24.8	2.7	3120	NO	cis
t-Bu	I	+27.5	24.8	2.7	2273	NO	trans
Ph	I	−2.5	5.6	8.1	3125	−343	cis
Bzl	I	−3.0	9.1	12.1	3157	−348	cis
Bzl	I	−3.0	8.5	11.5	2267	−438	trans

L = Phosphine

phosphine	X	$\delta(^{31}P_{ligand})$	$\delta(^{31}P_{complex})$	$\Delta\delta(^{31}P)$[b]	$^1J_{PtP}$[a]	$\delta(^{195}Pt)$[c]	geometry
Bzl_3P	Cl	−12.9	4.7	17.6	3652	185	cis
Bzl_3P	Cl	−12.9	5.3	18.2	2462	553	trans
Bzl_2PhP	Cl	−12.1	8.4	20.5	2534	543	trans
$BzlPh_2P$	Cl	−10.4	9.0	19.4	3735	109	cis
n-Bu_3P	Cl	−32.8	0.1	32.7	3508	81	cis
Et_3P	Cl	−20.4	8.6	29.0	3509	43	cis
Et_3P	Cl	−20.4	−0.4	20.0	2400	588	trans
Me_3P	Cl	−62.5	−25.1	37.4	3481	125	cis
Me_2PhP	Cl	−46.9	−15.8	31.1	3550	130	cis
Me_2PhP	Br	−46.9	−15.8	31.1	3506	−113	cis
Me_2PhP	I	−46.9	−18.0	28.9	3374	−149	cis
Me_2PhP	I	−46.9	−23.6	23.3	2312	−595	trans
$MePh_2P$	Cl	−28.2	−2.6	25.6	3621	96	cis
$MePh_2P$	Br	−28.2	9.8	38.0	3576	−165	cis
$MePh_2P$	I	−28.2	7.2	35.4	3435	236	cis
$MePh_2P$	I	−28.2	4.4	32.6	2392	−203	trans

[a] In hertz. [b] $\Delta\delta(^{31}P) = \delta(^{31}P_{complex}) - \delta(^{31}P_{ligand})$. [c] Data were obtained at 50-kHz sweep width, 8K data points, and 12.2-Hz data-point resolution. Consequently, uncertainties are of this magnitude.

Table VI. Coordination Chemical Shift Equations: $\Delta\delta(^{31}P) = A[\delta(^{31}P_{\text{ligand}})] + B$

L = 1-R-3,4-dimethylphospholes	A	B	r^a
cis-L_2PtCl_2	−0.110	14.06	0.66
cis-L_2PtBr_2	−0.411	11.37	0.97
cis-L_2PtI_2	−0.283	9.35	0.95
L_3PtCl_2			
triplet	−0.345	12.38	0.91
doublet	−0.779	39.61	0.83
L_3PtBr_2			
triplet	−0.380	13.30	0.92
doublet	−0.733	35.79	0.82
L_3PtI_2			
triplet	−0.346	11.41	0.99
doublet	−0.449	35.14	0.32

[a] The correlation coefficient.

giving rise to the familiar ^{195}Pt "satellites". Hence, one observes a pseudotriplet with relative intensities of 1:4:1 in the $^{31}P\{^1H\}$ NMR of either isomer with $^1J_{PtP}$ being the separation of the two outer lines of the pseudotriplet. The $^{195}Pt\{^1H\}$ NMR spectrum exhibits first-order triplets for each isomer (^{31}P, $I = ^1/_2$, 100% abundance) with $^1J_{PtP}$ being the separation of the lines in the triplet. The resonance due to the trans isomer is found upfield of that of the cis isomer for both ^{31}P and ^{195}Pt nuclei. Platinum–phosphorus coupling constants of the cis isomers are significantly greater (>3000 Hz) than those of the trans isomers (<2400 Hz), and this is consistent with previous NMR observations[33,34] of Pt(II)–phosphine complexes. The smaller downfield chemical shifts and small Pt–P coupling constants in the trans complexes relative to those in the cis complexes are manifestations of the weaker Pt–P bonds in the trans complexes as a result of the large trans influence[35] of the phospholes. The magnitude of the difference in these parameters for the cis and trans phosphole complexes is the same as that observed for typical phosphine complexes. This suggests that platinum–phosphole and platinum–phosphine bonds have similar strengths.

For each of the chloride, bromide, and iodide series of L_2PtX_2 complexes, a linear relationship is exhibited between the coordination chemical shift, $\Delta\delta(^{31}P)$, and the free-ligand chemical shift, $\delta(^{31}P_{\text{ligand}})$, of the form $\Delta\delta(^{31}P) = A[\delta(^{31}P)] + B$ as illustrated in Table VI. The phosphorus coordination chemical shift is indicative of the amount of electron density on phosphorus in the complex, and when chloride is replaced by bromide or iodide, we observe a decrease in $\Delta\delta(^{31}P)$ in the order Cl > Br > I. This occurs for Pd(II)–phosphole complexes[28] as well as for Pt(II)–trialkylphosphine complexes[36] and has been attributed to the increasing trans influence of the heavier halides, which allows for progressively less phosphorus σ donation. As a result, the coordinated phosphole has a character more like that of the free ligand as the halide trans to its becomes a better σ donor. In addition, $^1J_{PtP}$ decreases in the order Cl > Br > I for the same reason, and both of these trends are wholly consistent with each other and the trans influence.

Close examination of the NMR data reveals that the 1-R-3,4-dimethylphospholes exhibit ligand behavior that is significantly different from that of phosphines, and the following observations may be made concerning this behavior.

(A) $^1J_{PtP}$ is smaller for phosphole complexes than for analogous phosphine complexes. This is best illustrated by comparing the data for the $[(CH_3)_2PC_6H_5]_2PtX_2$ complexes with those for (1-phenyl-3,4-dimethylphosphole)$_2$PtX$_2$ complexes (Table V). A smaller value of $^1J_{PtP}$ in the phosphole complexes points to less s character and therefore more p character in the platinum–phosphole bond than in the platinum–phosphine bond and suggests that the phosphole is more electronegative than the phosphine in agreement with Bent's rules.[37] This idea is supported by the observation that, upon coordination, the change in $^1J_{PC}$(phenyl) for 1-phenyl-3,4-dimethylphosphole is more positive ($\Delta J_{PC} = +59.2$) than that observed for dimethylphenylphosphine ($\Delta J_{PC} = +52.5$), indicating more s character in the phosphole phosphorus–carbon bonds and therefore more p character in the phosphole phosphorus–platinum bond.

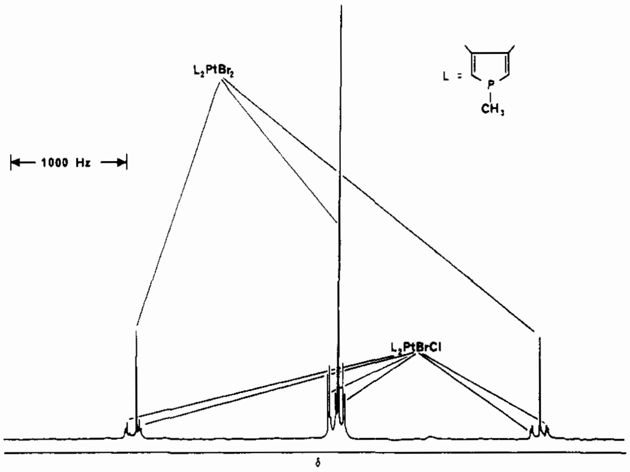

Figure 3. $^{31}P\{^1H\}$ NMR of L_2PtBr_2 and $L_2PtBrCl$ (L = 1,3,4-trimethylphosphole) in CH_2Cl_2 at 300 K.

(B) In the correlations of the coordination chemical shifts (Table VI) the values of B represent an average coordination chemical shift. For Pt(II)–phosphole complexes this value is generally less than that found for similar Pt(II)–phosphine complexes (vide infra). Thus, upon coordination, there is less of an apparent change in electron density on the phosphole phosphorus than on the phosphine phosphorus. In addition, the phosphole ring α carbons (Table IV) are more shielded for the coordinated ligand than for the free ligand,[38] while the remaining carbons become deshielded upon coordination. By comparison, the methyl carbons of dimethylphenylphosphine become deshielded upon coordination to platinum($\Delta\delta(^{13}C) = +0.9$). The shielding of the phosphole ring α carbons upon coordination is most likely largely the result of a polarization of the phosphole C=C double bonds due to the increase of the positive charge on phosphorus upon coordination.[27] This same effect was observed in the $^{13}C\{^1H\}$ NMR spectra of the analogous palladium complexes.[28]

(C) Within each halide grouping, $\delta(^{195}Pt)$ correlates linearly with $\Delta\delta(^{31}P)$ ($r = 0.92$). In this correlation the complex with the smallest value for $\Delta\delta(^{31}P)$ has the most bulky ligand[28] and the most shielded platinum nucleus. The values of $\Delta\delta(^{13}C)$ for the ring α carbons also show that the complex with the bulkiest ligand has the least shielded α carbons relative to those of the free ligand. A bulky substituent would not allow a relatively close approach to platinum, resulting in a weakened platinum–phosphorus bond.

(D) Superficially, the trend for $^1J_{PtP}$ within a given halide grouping does not support the π-bonding argument. However, $^1J_{PtP}$ primarily reflects the s character in the Pt–P bond, and as such, the trend results from a combination of steric and electronic effects of the exocyclic substituent R.

---

(33) Pidcock, A.; Richards, R. E.; Venanzi, L. M. *Proc. Chem. Soc., London* **1962**, 184.

(34) Grim, S. O.; Keiter, R. L.; McFarlane, W. *Inorg. Chem.* **1967**, *6*, 1133.

(35) Pidcock, A.; Richards, R. E.; Venanzi, L. M. *J. Chem. Soc. A* **1966**, 1707.

(36) Mather, G. G.; Rapsey, G. J. N.; Pidcock, A. *Inorg. Nucl. Chem. Lett.* **1973**, *9*, 567.

(37) Bent, H. A. *Chem. Rev.* **1961**, *61*, 275.

(38) Gray, G. A.; Nelson, J. H. *Org. Magn. Reson.* **1980**, *14*, 14.

Table VII. ^{31}P and ^{195}Pt NMR Data for the (1-R-3,4-dimethylphosphole)$_n$PtBrCl Complexes

R	*n*	$\delta(^{31}P)^a$	$^2J_{PP}$	$^1J_{PtP}$	$\delta(^{31}P)^b$	$^1J_{PtP}$	$\delta(^{195}Pt)^c$	geometry
CH_3	2	0.3	17.1	3269	−4.3	3254	+2	cis
n-Bu	2	11.3	17.1	3273	7.0	3268	−47	cis
t-Bu	2	19.0	14.7	3273	26.0	3287	−149	cis
Ph	2	9.8	18.3	3320	6.1	3312	−102	cis
Bzl	2	13.4	14.7	3352	9.7	3352	−63	cis
CH_3	3	16.3	19.6	2148	−2.4	3154	−248	sbp[d]
n-Bu	3	24.27	22.0	2141	9.32	3140	−285	sbp
t-Bu	3	40.2	19.5	2185	30.2	3217	−371	sbp
Ph	3	24.4	22.0	2251	9.6	3130	−309	sbp
Bzl	3	29.3	17.0	2222	15.2	3379	−336	sbp

[a] Trans to Cl; all complexes were in CH_2Cl_2 solution at 25 °C. Positions are relative to external 85% H_3PO_4 with downfield positions positive. [b] Trans to Br. [c] Data were obtained at 50-kHz sweep width with 8K data points and 12.2-Hz data-point resolution. Consequently, uncertainties are of this magnitude. [d] sbp ≡ square-based pyramid.

As mentioned earlier, care must be taken to allow sufficient reaction time when preparing L_2PtBr_2 and L_2PtI_2 by metathesis of L_2PtCl_2 as these reactions are slow. Crystalline materials were isolated from the reactions of L_2PtCl_2 with NaBr, which, when dissolved in CH_2Cl_2, gave $^{31}P\{^1H\}$ and $^{195}Pt\{^1H\}$ NMR spectra (Table VII) that suggested that these materials were a mixture of $L_2PtClBr$ and L_2PtBr_2. The $L_2PtClBr$ species exhibited two doublets with accompanying ^{195}Pt "satellites" (Figure 3) in their $^{31}P\{^1H\}$ NMR, establishing that these complexes possessed the cis geometry with two phosphorus nuclei in magnetically different environments, one trans to chloride and one trans to bromide. If these solutions contained a mixture of L_2PtCl_2 and L_2PtBr_2, we would observe two singlets in the ^{31}P NMR with accompanying ^{195}Pt satellites regardless of the geometry of the L_2PtCl_2 and L_2PtBr_2 complexes. The magnitude of the Pt–P coupling constants would distinguish cis ($J_{PtP} > 3000$ Hz) from trans ($J_{PtP} < 2400$ Hz). If $L_2PtBrCl$ possessed the trans geometry, its ^{31}P NMR spectrum would also be a singlet with ^{195}Pt satellites and for it $^1J_{PtP}$ should be intermediate between the values of *trans*-L_2PtBr_2 and *trans*-L_2PtCl_2 and be in the vicinity of 2000 Hz. We observed no trans isomers in these solutions, as values of $^1J_{PtP}$ ranged from 3254 to 3352 Hz. The platinum–phosphorus coupling constants for the magnetically inequivalent phospholes in *cis*-$L_2PtBrCl$ reflect the difference in the trans influence of bromide and chloride, with J_{PtP} for the phosphole trans to chloride being greater than J_{PtP} for the phosphole trans to bromide, typically by 5–10 Hz. Values of $\delta(^{195}Pt)$ (Table VII) are intermediate between those of *cis*-L_2PtCl_2 and *cis*-L_2PtBr_2 as would be expected.[30]

These data clearly establish that bromide substitution of chloride is stereospecific for these complexes in both steps of reaction 1 and is a good example of the trans effect in operation.

$$cis\text{-}L_2PtCl_2 \underset{+Cl^-}{\overset{+Br^-}{\rightleftharpoons}} cis\text{-}L_2PtBrCl \underset{+Cl^-}{\overset{+Br^-}{\rightleftharpoons}} cis\text{-}L_2PtBr_2 \quad (1)$$

II. Five-Coordinate Complexes. Addition of excess phosphole to CH_2Cl_2, $CDCl_3$, or CH_3OH solutions or L_2PtX_2 causes a change from pale yellow to deep red, and the resulting solutions show nonelectrolyte behavior (no measurable conductance). At 25 °C the $^{31}P\{^1H\}$ NMR in either CH_2Cl_2 or $CDCl_3$ shows that rapid intra- and intermolecular exchange is occurring, as only broad resonances are observed at 25 °C. When these solutions are cooled to −50 °C, A_2X ^{31}P NMR spectra are observed (Table VIII) with a downfield doublet arising from two mutually trans phosphorus nuclei and an upfield triplet representing the unique phosphorus nucleus, which is cis to the other two phospholes (Figure 4). For the L_3PtX_2 complexes, phosphorus shielding of the mutually trans phospholes increases in the order Cl < Br < I and mimics the behavior of the four-coordinate complexes. The shielding of the remaining phosphole varies in the order Br < Cl < I.

Table VIII. ^{31}P and ^{195}Pt NMR Data for the (1-R-3,4-dimethylphosphole)$_3$PtX$_2$ Complexes

R	X	*T*, K	$\delta(^{31}P)^a$	$^2J_{PP}$	$^1J_{PtP}$	$\delta(^{31}P)^a$	$^1J_{PtP}$	$\delta(^{195}Pt)^b$
CH_3	Cl	203	15.7 d	19.5	2153	−2.9 t	3159	−247
n-Bu	Cl	216	25.4 d	19.5	2143	7.8 t	3154	−282
t-Bu	Cl	216	40.1 d	19.5	2196	29.2 t	3234	−344
Ph	Cl	203	24.3 d	22.0	2246	9.5 t	3127	−308
Bzl	Cl	203	29.4 d	19.5	2246	15.2 t	3310	−300
CH_3	Br	216	12.5 d	21.9	2125	−0.6 t	3130	−414
n-Bu	Br	216	21.6 d	19.6	2120	7.7 t	3125	−406
t-Bu	Br	216	35.9 d	19.5	2178	29.4 t	3203	−496
Ph	Br	203	20.8 d	22.0	2231	10.8 t	3110	−491
Bzl	Br	203	26.0 d	19.0	2235	16.3 t	3291	−490
CH_3	I	216	5.4 d	22.0	2108	−1.8 t	3039	−244
Ph	I	205	14.4 d	22.0	2207	10.2 t	2993	−348
Bzl	I	203	19.8 d	19.5	2214	9.0 t	3159	−283

[a] All complexes were in CH_2Cl_2 solution. Positions are relative to external 85% H_3PO_4 with downfield positions positive; d = doublet, t = triplet. [b] Data obtained at 50-kHz sweep width with 8 K data points and 12.2-Hz data-point resolution. Consequently, uncertainties are of this magnitude.

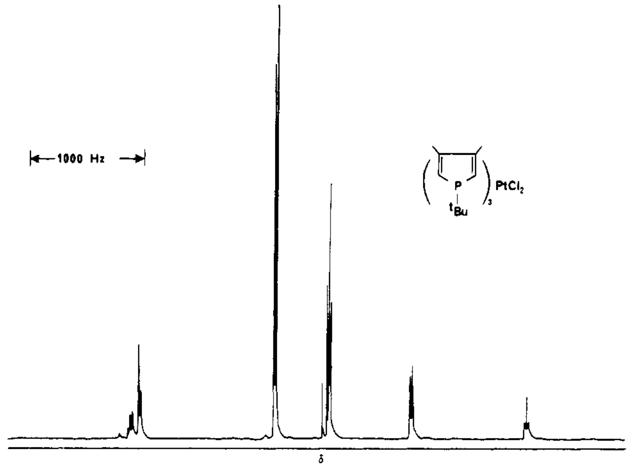

Figure 4. $^{31}P\{^1H\}$ NMR of (1-*tert*-butyl-3,4-dimethylphosphole)$_3$PtCl$_2$ at 216 K in CH_2Cl_2. The small resonance downfield of the triplet is due to *trans*-L_2PtCl_2.

Consistent with the $^{31}P\{^1H\}$ NMR, the $^{195}Pt\{^1H\}$ NMR spectra of these solutions at −50 °C (Table VIII) are first-order doublets of triplets. For L_3PtX_2, $\delta(^{195}Pt)$ is more shielded than $\delta(^{195}Pt)$ for L_2PtX_2 as one might expect for the addition of another phosphole, and $\delta(^{195}Pt)$ for L_3PtX_2 increases in the order I < Cl < Br. For both types of phospholes in L_3PtX_2, $^1J_{PtP}$ decreases in the order Cl > Br > I, and within a given halide grouping there is no apparent trend.

As illustrated in Figure 5 a CH_2Cl_2 solution of an equimolar mixture of 1-phenyl-3,4-dimethylphosphole (L) and L_2PtCl_2 contains a temperature-dependent equilibrium mixture of

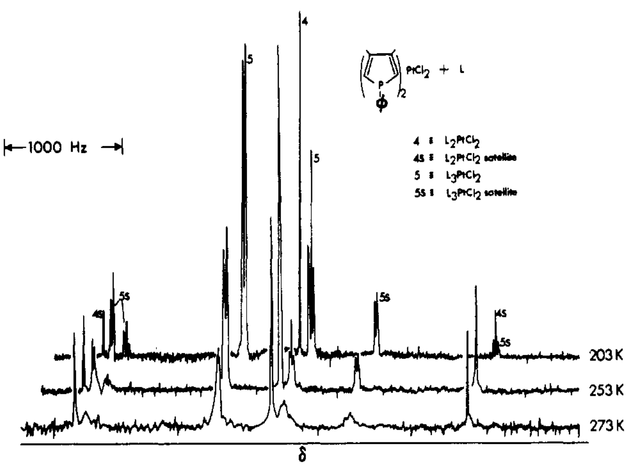

Figure 5. Variable-temperature $^{31}P\{^1H\}$ NMR of a 1:1 molar mixture of (1-phenyl-3,4-dimethylphosphole)$_2$PtCl$_2$ and free phosphole in CH_2Cl_2.

Table IX. Equilibrium Thermodynamics for the Reaction

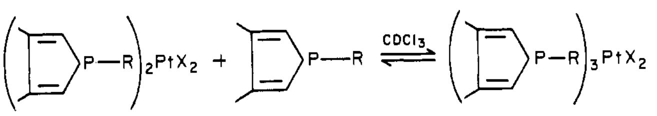

R	X	ΔG_{300}, kcal/mol	ΔH, kcal/mol[a]	ΔS, eu[b]	T_{intra}, K[c]	T_{inter}, K[c]
t-C_4H_9	Cl	1.28	−3.0	−14.2	~293	~318
t-C_4H_9	Br	1.65	−4.1	−19.0	~303	>333
C_6H_5	Cl	0.69	−2.4	−10.2	~263	~303
C_6H_5	Br	1.53	−2.6	−13.7	~270	~303

[a] The uncertainties in ΔG and ΔH are believed to be 0.5 kcal/mol. [b] The uncertainty in ΔS is believed to be 1 eu. [c] Approximate coalescence temperatures for intramolecular exchange within L_3PtX_2 (T_{intra}) and intermolecular exchange between L_3PtX_2, L_2PtX_2, and L (T_{inter}).

L_3PtCl_2, *cis*-L_2PtCl_2, and L (although no free L is detected by ^{31}P NMR, and this phenomenon has been previously observed[26]). The L_3PtCl_2 complexes are stereochemically nonrigid in CH_2Cl_2 in the temperature range 203–263 K, and they slowly equilibrate with *cis*-L_2PtCl_2 in solution. The exchange of L_3PtCl_2 is largely intramolecular over this temperature range as spin correlation of platinum and phosphorus nuclei is maintained. Above 263 K intramolecular rearrangement of L_3PtCl_2 becomes increasingly rapid as evidenced by the loss of ^{31}P–^{31}P coupling, while intermolecular exchange does not become rapid until 303 K, where the respective $^{31}P\{^1H\}$ resonances coalesce.

The temperature dependence of the $^{31}P\{^1H\}$ NMR pertinent to the equilibrium $L_2PtX_2 + L \rightleftharpoons L_3PtX_2$ for four sets of complexes is described by the thermodynamic quantities listed in Table IX. These data show that the formation of L_3PtX_2 from L_2PtX_2 is enthalpy favored and entropy disfavored when L = phosphole II. This suggests to us that the steric bulk of L is very important in determining the stability of L_3PtX_2 complexes.

The relative solution dynamics also depend on L, as indicated by the approximate coalescence temperatures for intra- and intermolecular ligand exchange (Table IX). These findings are in agreement with previous observations,[39] which indicate that the rate of intramolecular exchange in pentacoordinate compounds is inversely proportional to ligand bulk. The L_3PtX_2 phosphole complexes are thermodynamically less stable, are more labile toward intermolecular ligand exchange, and exhibit greater stereochemical rigidity than do the isoleptic $[L'_5Pt]^{2+}$ complexes, where L′ is a phosphite.[39] This is most likely due to the phosphole's steric nature as it is clear that phospholes have a much larger Tolman cone angle than phosphites due to their relatively large CPC exocyclic angle (106° in 1-benzylphosphole).

If the CH_2Cl_2 is evaporated from the above solutions and the residue is dissolved with filtering into CH_3OH, $^{31}P\{^1H\}$ and $^{195}Pt\{^1H\}$ NMR spectra of the CH_3OH solutions are the same in CH_3OH at 299 K as they were in CH_2Cl_2 at 223 K. The pentacoordinate species are therefore considerably more rigid in CH_3OH solution than in CH_2Cl_2 solution. It was anticipated that the higher dielectric solvent (methanol) would promote the formation of the ionic species $[L_3PtX]^+X^-$ from L_3PtX_2, but the methanol solutions have no conductance. In addition the mixtures containing $L_3PtClBr$ and L_3PtBr_2 show no anion scrambling in either methanol or dichloromethane; the $^{31}P\{^1H\}$ and $^{195}Pt\{^1H\}$ NMR clearly show the existence of both species in methanol.

Louw recently concluded[16] that intramolecular ligand exchange must be faster than intermolecular ligand exchange for cis–trans isomerization to occur through a pentacoordinate state, and this tenet is supported by the data for the phosphole L_2PtX_2 complexes. However, his statement that "isomerization in the platinum halide–phosphine square-planar system tends to proceed when a stable five-coordinate intermediate can be formed" must be reconsidered. Each of the four phosphole complexes studied is cis at room temperature in the absence of excess ligand, yet only the complex that forms the least thermodynamically stable and most rigid L_3PtX_2 species (L = 1-*tert*-butyl-3,4-dimethylphosphole, X = Br^-) isomerizes in the presence of excess phosphole. We suggest that when the energy difference between cis and trans complexes is great, phosphorus ligand-catalyzed cis–trans isomerism will not occur; rather, an equilibrium between *cis*-L_2PtX_2 and L_3PtX_2 will be established (Figure 6). The energy differences among the various species are likely due to a combination of ligand steric and electronic effects, which will affect the relative energies of all species in Figure 6. This rationalizes Haake's observations[4] regarding the lack of ligand exchange in the phosphine-catalyzed isomerization of $(R_3P)_2PtX_2$ complexes—conditions can arise where the ligand is small enough to allow formation of a pentacoordinate species but large enough to give a sizeable barrier to pseudorotation. Hence, when L_3PtX_2 species are not stable enough to form as intermediates, any of the three mechanisms (Figure 7) can occur and solvent will probably dictate which is operational: polar solvents[10,16] favor the consecutive neutral-ligand displacement. The validity of Haake's postulate of a unique coordination site for the catalyzing ligand will therefore depend on the nature of that ligand. His failure to observe ligand exchange is not surprising—while $LL'MX_2$ complexes might be more stable in solution than symmetric L_2MX_2 complexes,[40] this is generally not so in the solid state.[41] We believe that only in rare cases will the pseudorotation mechanism dominate.

After this study was completed, Favez and Roulet[42] independently reached similar conclusions regarding the likelihood

---

(39) Jesson, J. P.; Muetterties, E. L. "Dynamic Nuclear Magnetic Resonance Spectroscopy"; Jackman, L. M., Cotton, F. A., Eds.; Academic Press: New York, 1975; p 253 ff.

(40) Verstuyft, A. W.; Redfield, D. A.; Cary, L. W.; Nelson, J. H. *Inorg. Chem.* **1976**, *15*, 1128.

(41) Haake's proposal of the unique coordination site rests upon his inability to isolate mixed-ligand complexes of the type $LL'MX_2$ from solutions of L_2MX_2 and L′. Several examples of the formation of $L'LMX_2$ in solution have been reported,[40] which show that in solution the equilibrium $L_2MX_2 + L'_2MX_2 \rightleftharpoons 2LL'MX_2$ favors the $LL'MX_2$ species. In each of these reported cases, if the solution is allowed to slowly evaporate, the symmetric L_2MX_2 and L'_2MX_2 complexes crystallize. This is a very clear example of a marked difference in solution and solid-state stabilities.

(42) Favez, R.; Roulet, R. *Inorg. Chem.* **1981**, *20*, 1598.

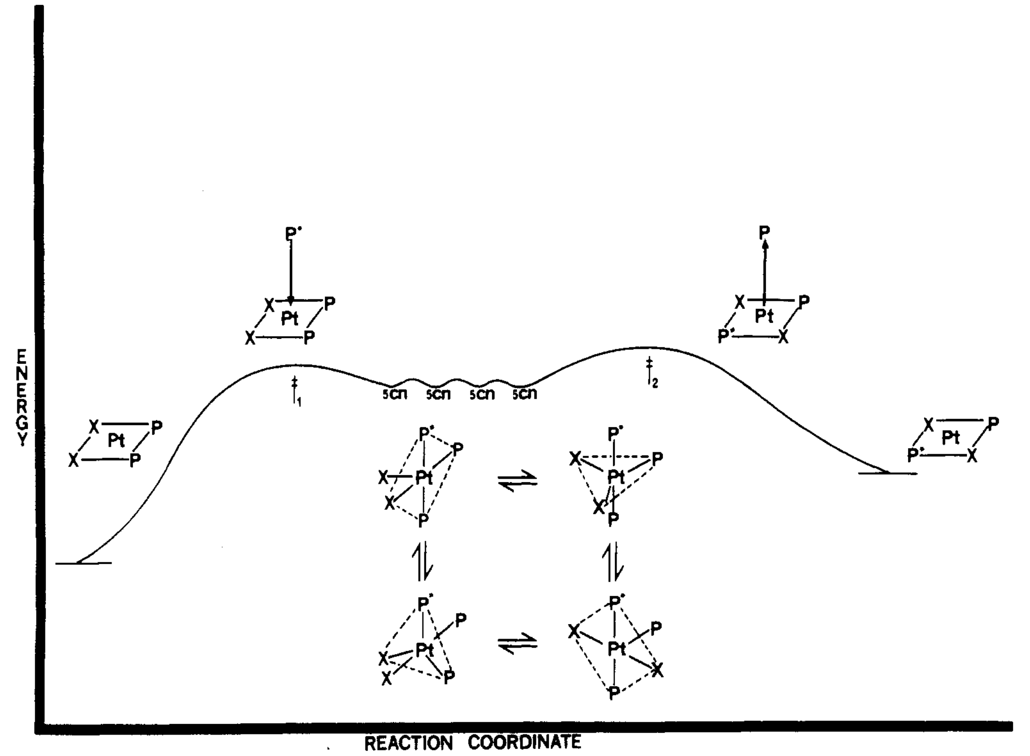

Figure 6. Pseudorotation mechanism energy profile.

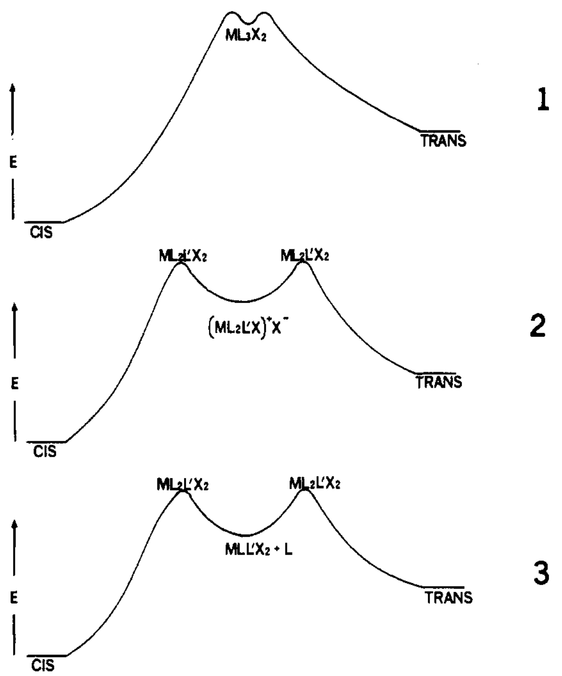

Figure 7. Energy profiles for isomerization mechanisms of L_2MX_2: (1) pseudorotation, (2) consecutive anion displacement, and (3) consecutive neutral-ligand displacement. The energies of the $ML_2L'X_2$ species need not be the same, but they probably will not differ by more than vibrational energy differences.

of the pseudorotation mechanism. Their conclusions are, however, stronger than ours. They state "there is no evidence that a Berry-type pseudorotation is a low-activation-energy process in ML_3X_2 (M = Pd,Pt)". Our data suggest that Berry pseudorotation does have a low-activation-energy barrier for the phosphole complexes, but it generally does not result in geometrical isomerization of L_2PtX_2 (L = phosphole) complexes.

Experiments similar to those described above were performed with Pd(II) phosphole complexes, and the observed pentacoordinate species were uniformly less stable and less rigid than their platinum counterparts. With the exception of one complex, cis–trans isomerization was not observed in the platinum(II) system upon addition of excess phosphole. In contrast, addition of excess ligand readily catalyzed cis–trans isomerization for each of the Pd(II) complexes studied, with only very small amounts of L_3PdX_2 being detected. The equilibrium thermodynamical values calculated for these solutions are in agreement with those previously obtained[29] for solutions containing only L_2PdX_2.

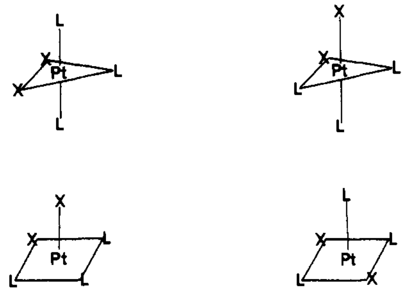

Figure 8. Possible structures of L_3PtX_2 complexes that are consistent with the spectroscopic data. On the basis of three crystal structures for L'_3PdX_2 complexes,[44] we favor the square-based-pyramidal geometry.

Recently, Pfeiffer demonstrated[43] carbon monoxide catalyzed isomerization of *cis*-$PtCl_2(n\text{-}Bu_3P)_2$, and we attempted to achieve the same results with our *cis*-(phosphole)$_2PtX_2$ complexes. When CO was bubbled through CH_2Cl_2 solutions of these complexes, no color change occurred, no coordinated CO could be detected by IR spectroscopy, and the $^{31}P\{^1H\}$ NMR spectra of these solutions were identical with those of *cis*-L_2PtX_2.

The A_2X pattern displayed in the low-temperature $^{31}P\{^1H\}$ NMR spectrum of the L_3PtX_2 species (Figure 4) is consistent with two trigonal-bipyramid and two square-base-pyramid configurations (Figure 8). The ionic complex $[L_3PtX]^+X^-$

---

[43] Pfeiffer, R. M. *Synth. React. Inorg. Met.-Org. Chem.* **1976**, *6*, 55.

would also give an A_2X pattern; however, the NMR data for the mixed-anion complexes and conductance data (vide supra) rule this out. Hypothetically, upon addition of excess ligand L to L_2PtCl_2 and to L_2PtBr_2, we could possibly observe L_3PtCl_2, L_3PtBr_2, $[L_3PtCl]^+Cl^-$, or $[L_3PtBr]^+Br^-$. Similarly, we would expect the addition of L to $L_2PtClBr$ to give $L_3PtClBr$, $[L_3PtCl]^+Br^-$, or $[L_3PtBr]^+Cl^-$. These last two forms would give $^{31}P\{^1H\}$ and $^{195}Pt\{^1H\}$ NMR spectra essentially identical with those for the dichloro and dibromo species, if ionic compounds were being formed in these cases. The results in Table VII exclude the possibility of ionic complexes as the NMR spectra of $L_2PtClBr$ + L are substantially different from those of either L_2PtCl_2 + L or L_2PtBr_2 + L. NMR spectroscopy alone cannot unambiguously determine the geometry of L_3MX_2 species in solution, since the same A_2X pattern is expected for each of the four configurations (Figure 8). The solution geometries of the complexes are most likely distorted between SBP and TBP, consistent with the limited amount of structural data[44] for L_3MX_2 complexes.

Acknowledgment. The financial support of the University of Nevada, Reno, Research Advisory Board is gratefully acknowledged. We are grateful to the National Science Foundation (Grant No. CHE77-08937) for providing funds to purchase the Fourier transform NMR spectrometer. Helpful discussions with Professor H. E. LeMay are greatly appreciated.

Registry No. *cis*-L_2PtX_2, R = CH_3, X = Cl, 81011-50-9; *cis*-L_2PtX_2, R = *n*-Bu, X = Cl, 81011-51-0; *cis*-L_2PtX_2, R = *t*-Bu, X = Cl, 81011-52-1; *cis*-L_2PtX_2, R = Bzl, X = Cl, 81011-53-2; *cis*-L_2PtX_2, R = Ph, X = Cl, 81011-54-3; *cis*-L_2PtX_2, R = CH_3, X = Br, 81011-55-4; *cis*-L_2PtX_2, R = *n*-Bu, X = Br, 81011-56-5; *cis*-L_2PtX_2, R = *t*-Bu, X = Br, 81011-57-6; *cis*-L_2PtX_2, R = Bzl, X = Br, 81011-58-7; *cis*-L_2PtX_2, R = Ph, X = Br, 81027-52-3; *cis*-L_2PtX_2, R = CH_3, X = I, 81011-59-8; *trans*-L_2PtX_2, R = CH_3, X = I, 81075-66-3; *cis*-L_2PtX_2, R = *n*-Bu, X = I, 81011-60-1; *trans*-L_2PtX_2, R = *n*-Bu, X = I, 81011-61-2; *cis*-L_2PtX_2, R = *t*-Bu, X = I, 81075-67-4; *cis*-L_2PtX_2, R = Bzl, X = I, 81011-62-3; *trans*-L_2PtX_2, R = Bzl, X = I, 81075-68-5; *cis*-L_2PtX_2, R = Ph, X = I, 81011-63-4; *cis*-$L_2PtBrCl$, R = CH_3, 81011-64-5; *cis*-$L_2PtBrCl$, R = *n*-Bu, 81011-65-6; *cis*-$L_2PtBrCl$, R = *t*-Bu, 81011-66-7; *cis*-$L_2PtBrCl$, R = Ph, 81011-67-8; *cis*-$L_2PtBrCl$, R = Bzl, 81011-68-9; $L_3PtBrCl$, R = CH_3, 81011-69-0; $L_3PtBrCl$, R = *n*-Bu, 81011-70-3; $L_3PtBrCl$, R = *t*-Bu, 81011-71-4; $L_3PtBrCl$, R = Ph, 81011-72-5; $L_3PtBrCl$, R = Bzl, 81011-73-6; L_3PtCl_2, R = *t*-Bu, 81011-74-7; *cis*-L_2PtX_2, L = Bzl_3P, X = Cl, 81075-69-6; *trans*-L_2PtX_2, L = Bzl_3P, X = Cl, 63902-66-9; *trans*-L_2PtX_2, L = Bzl_2PhP, X = Cl, 63848-36-2; *cis*-L_2PtX_2, L = $BzlPh_2P$, X = Cl, 61586-06-9; *cis*-L_2PtX_2, L = Bu_3P, X = Cl, 15390-92-8; *cis*-L_2PtX_2, L = Et_3P, X = Cl, 15692-07-6; *trans*-L_2PtX_2, L = Et_3P, X = Cl, 13965-02-1; *cis*-L_2PtX_2, L = Me_3P, X = Cl, 15630-86-1; *cis*-L_2PtX_2, L = Me_2PhP, X = Cl, 15393-14-3; *cis*-L_2PtX_2, L = Me_2PhP, X = Br, 15616-81-6; *cis*-L_2PtX_2, L = Me_2PhP, X = I, 41119-52-2; *trans*-L_2PtX_2, L = Me_2PhP, X = I, 4119-53-3; *cis*-L_2PtX_2, L = $MePh_2P$, X = Cl, 16633-72-0; *cis*-L_2PtX_2, L = $MePh_2P$, X = Br, 52613-13-5; *cis*-L_2PtX_2, L = $MePh_2P$, X = I, 28425-03-8; *trans*-L_2PtX_2, L = $MePh_2P$, X = I, 28425-02-7.

---

[44] Louw, W. J.; deWaal, D. J. A.; Kruger, G. J. *J. Chem. Soc., Dalton Trans.* **1976**, 2364. Chui, K. M.; Powell, H. M. *Ibid.* **1974**, 2117. Chui, K. M.; Powell, H. M. *Ibid.* **1974**, 1879.

Contribution from the Kenan Laboratories of Chemistry,
The University of North Carolina, Chapel Hill, North Carolina 27514

Electropolymerization of Vinylpyridine and Vinylbipyridine Complexes of Iron and Ruthenium: Homopolymers, Copolymers, Reactive Polymers

P. DENISEVICH, H. D. ABRUÑA, C. R. LEIDNER, T. J. MEYER,* and ROYCE W. MURRAY*

Received July 10, 1981

Electroreductive polymerizations of the vinyl-substituted monomer complexes $[Ru(vbpy)_3]^{2+}$, $[Fe(vbpy)_3]^{2+}$, $[Ru(bpy)_2(vpy)_2]^{2+}$, $[Ru(bpy)_2(vpy)Cl]^+$, $[Ru(vbpy)_2Cl_2]$, $[Ru(bpy)_2(vpy)NO_2]^+$, and $[Ru(bpy)_2(vbpy)]^{2+}$ are described, where vbpy = 4-vinyl-4′-methyl-2,2′-bipyridine and vpy = 4-vinylpyridine. The polymers form stable, adherent, electrochemically reactive films on the reducing electrode, which can be Pt, Au, vitreous carbon, SnO_2, or TiO_2. Complexes with only one vinyl substituent are difficult to polymerize but can be copolymerized with divinyl- and trivinyl-substituted monomers. The possibility that the polymers are in part metal macroclusters with bridging ligands is discussed. Films containing from 4 to ca. 1500 monolayers of metal complex can be formed depending on the potential control conditions employed during polymerization. Charge transport through poly-$[Ru(vbpy)_3]^{2+}$ films occurs with $D_{ct} = 2 \times 10^{-10}$ cm²/s, which corresponds to an apparent $[Ru(vbpy)_3]^{3+/2+}$ electron-self-exchange rate in the film of 1.7×10^5 M^{-1} s^{-1}. Quantitative reactivity of ruthenium centers in this film was demonstrated with use of spectrophotometry of films on SnO_2 electrodes, and composition was evaluated by X-ray photoelectron spectroscopy. The cross-linked, polycationic films are poorly permeable to cations and bulky, neutral molecules dissolved in the contacting solution but readily incorporate small anions. Chemical reactivity of poly-$[Ru(bpy)_2(vpy)NO_2]^+$ is somewhat altered by the polymeric environment as compared to that of prior monolayer studies.

Binding of transition-metal complexes to preformed, ligand-containing polymers[1,2] typically results, for steric and/or electrostatic reasons, in incomplete metalation of the polymeric ligand sites. This has been the case in recent studies involving the coating of electrodes with cobalt and ruthenium complexes bound to polyvinylpyridine.[2b,3-7]

We recently described[8] the coating of electrodes by the reductive, electrochemical polymerization of several vinylpyridine and vinylbipyridine complexes of iron and ruthenium. The use of vinyl-substituted metal complexes as monomers offers the possibility of preparing polymeric films with essentially complete metalation of ligand sites and a well-defined coordination environment for the metal. Since the monomer metal complex approach to electroactive polymer films is uncommon, we have carried out studies aimed at better understanding the ruthenium vinylpyridine and vinylbipyridine electropolymerizations and the possible generality of the chemistry involved. These studies have included relative ease

---

[1] Tsuchida, E.; Nischide, H. *Adv. Polym. Sci.* **1977**, *24*, 1.

[2] (a) Oyama, N.; Anson, F. C. *J. Am. Chem. Soc.* **1979**, *101*, 739. (b) *Ibid.* **1979**, *101*, 3450.

[3] Oyama, N.; Anson, F. C. *J. Electrochem. Soc.* **1980**, *127*, 247.

[4] Oyama, N.; Shimomura, T.; Shigehara, K.; Anson, F. C. *J. Electroanal. Chem. Interfacial Electrochem.* **1980**, *112*, 271.

[5] Haas, O.; Vos, J. G. *J. Electroanal. Chem. Inferfacial Electrochem.* **1980**, *113*, 139.

[6] Calvert, J.; Meyer, T. J. *Inorg. Chem.* **1981**, *20*, 27.

[7] Samuels, G. J.; Meyer, T. J. *J. Am. Chem. Soc.* **1981**, *103*, 307.

[8] Abruña, H. D.; Denisevich, P.; Umaña, M.; Meyer, T. J.; Murray, R. W. *J. Am. Chem. Soc.* **1981**, *103*, 1.